

# HARDNESS AND TENSILE STRENGTH STUDY ON A356 ALLOY MATRIX/NANO $\text{Al}_2\text{O}_3$ PARTICLE REINFORCED COMPOSITE

A. Mazahery<sup>1</sup>, H. Abdizadeh<sup>2\*</sup>, and H.R. Baharvandi<sup>3</sup>

<sup>1,2</sup> School of Metallurgy and Materials Engineering, University of Tehran, Tehran, Iran  
\*abdizade@ut.ac.ir

## ABSTRACT

In order to investigate the effect of nano-alumina on the microstructure and mechanical properties of Al/nano $\text{Al}_2\text{O}_3$  composite, an innovative method was used in stir casting to avoid agglomeration and segregation of particles. Different volume fraction of nano-alumina particles were incorporated into the aluminum A356 alloy by a mechanical stirrer and cylindrical specimens at different temperatures were cast and tested. The microstructural characterization of the composite samples showed uniform distribution of reinforcement, grain refinement of aluminum matrix, and presence of the minimal porosity. The effects of  $\text{Al}_2\text{O}_3$  particle content and casting temperature on the mechanical properties of the composites were investigated. Based on experiments, it was revealed that the presence of nano $\text{Al}_2\text{O}_3$  reinforcement led to significant improvement in hardness, UTS and ductility. This combination of enhancement in UTS and ductility exhibited by nano $\text{Al}_2\text{O}_3$  reinforced aluminum is due to uniform distribution of reinforcement and grain refinement of aluminum matrix.

**KEYWORDS:**  $\text{Al}_2\text{O}_3$ , aluminum, microstructure, mechanical properties, nanocomposite.

## 1. INTRODUCTION

Metal matrix composites (MMCs) represent a new generation of engineering materials in which a strong ceramic reinforcement is incorporated into a metal matrix to improve its properties including specific strength, specific stiffness, wear resistance, corrosion resistance and elastic modulus [1,2]. The particle-reinforced aluminum alloy composites which are among the most widely used composites materials, found to be potential materials because of their excellent physical, mechanical and tribological properties and also because of good combination of thermal conductivity and dimensional stability (low thermal expansion coefficient) [3-13]. The tensile and the compressive deformation behaviours of particle reinforced MMCs have been carried out both at room temperature and elevated temperatures. It was reported that the strength and the stiffness increase with decrease in particle size and increase in volume fraction. But there is a greater tendency of agglomeration with decrease in particle size in common methods, which again leads to reduction in strength [14, 15]. Normally, micro-ceramic particles are used to improve the yield and ultimate tensile strength of the metal. However, the ductility of the MMCs deteriorates with high ceramic particle concentration [16]. It is of interest to use nano-sized ceramic particles to strengthen the metal matrix, while maintaining good ductility, high temperature creep resistance and better fatigue [16, 17]. A variety of methods for producing MMCs have recently become available, including mechanical alloying [18], ball milling [19], nano-sintering [20], etc. For mechanical alloying, it normally involves mechanical mixing of metallic and ceramic powders or different metallic powders for fabrication of bulk. Mixing of nano-sized ceramic particles is lengthy, expensive, and energy consuming. Compared with mechanical alloying, melt processing which involves the stirring of ceramic particles into melts, has some important advantages such as better matrix-particle bonding, easier control of matrix structure, simplicity, low cost of processing and nearer

net shape. However, it is extremely difficult for the mechanical stirring method to distribute and disperse nano-scale particles uniformly in metal melts due to their large surface-to-volume ratio and their low wettability in metal melts, which easily induce agglomeration and clustering. In this study, a new method was successfully introduced to distribute and disperse nanoparticles into Al alloy melts, thus making the production of cast high-performance nano-sized particles reinforced aluminium matrix composite promising.

## 2. EXPERIMENTS

In this study, 356 aluminium alloy {(wt.%): 7.5 Si, 0.38 Mg, 0.02 Zn, 0.001 Cu, 0.106 Fe and Al (balance)} was used as the matrix material while the mixture of  $\text{Al}_2\text{O}_3$  (alumina) particles with average particle size of 50 nm and Al particles with average size of 16  $\mu\text{m}$  were used as the reinforcements. The powders were mixed in the ratio of  $\text{Al}/\text{Al}_2\text{O}_3=1.67$  and ball milled in isopropyl alcohol for 20 min using WC/CO balls. The mixture was then dried in a rotary vacuum evaporator, and passed through a 60 mesh screen. The powder mixtures were cold pressed under 200 MPa into samples having  $60\times 60\times 60\text{ mm}^3$  dimension. The compacted samples were crushed and then passed through 60 mesh screen. For manufacturing of the MMCs, 0.75, 1.5, 2.5, 3.5 and 5 vol. %  $\text{Al}_2\text{O}_3$  particles were used. The required amount of  $\text{Al}_2\text{O}_3$  was calculated according to the ratio of  $\text{Al}/\text{Al}_2\text{O}_3$ . The metal matrix composites have been produced by using a vortex method. Approximately, 450 g of Al-356 alloy was charged into the crucible made from graphite and heated up to three temperatures (800, 850, and 950 °C) above the alloy liquidus temperature for melting. The graphite stirrer fixed on the mandrel of the drilling machine was introduced into the melt and positioned just below the surface of the melt. Approximately, 1 g powder mixture was inserted into an aluminium foil by forming a packet. The packets were added into molten metal of crucible when the vortex was formed at every 20 s. The packet of mixture melted and the particles started to distribute around the alloy sample. It was stirred for 15 min at approximately 600 rev/min speed. Composite slurry was poured into preheated cast iron moulds. The composites were shaped in the form of cylinder of 14 mm outer diameter and height of 140 mm.

For microstructure study, specimens were prepared by grinding through 120, 400, 600, and 800 grit papers followed by polishing with 6  $\mu\text{m}$  diamond paste and etched with Keller's reagent (2 ml HF (48%), 3 ml HCl (conc.), 5 ml  $\text{HNO}_3$  (conc.) and 190 ml water). Microscopic examinations of the composites and matrix alloy were carried out using a (CAMSCAN-MV2300 MODEL, OXFORD) scanning electron microscope (SEM). Image analysis was carried out to determine the grain size of the material. To study the hardness, The Brinell hardness values of the samples were measured on the polished samples using a ball with 2.5 mm diameter at a load of 31.25 kg. For each sample, 5 hardness readings on randomly selected regions were taken in order to eliminate possible segregation effects and get a representative value of the matrix material hardness. During hardness measurement, precaution was taken to make indentation at a distance of at least twice the diagonal length of the previous indentation. The tensile tests were used to assess the mechanical behaviour of the composites and matrix alloy. The composite and matrix alloy rods were machined to tensile specimens according to ASTM.B 557 standard. The load displacement diagram and the load displacement data were recorded from the digital display attached with the equipment.

These load and displacement data were transformed to true stress and true strain data using the standard methodology, and ultimate tensile strength values were obtained. Each value of ultimate tensile strength is an average of at least three tensile specimens.

### 3. RESULTS

Figure 1 shows the typical SEM micrographs of composites. Figure 1(a) displays the existence of some 1-2  $\mu\text{m}$   $\text{Al}_2\text{O}_3$  agglomerates in the matrix in low magnification. Figure 1(b) which is taken by using high magnification, indicates that nano-sized  $\text{Al}_2\text{O}_3$  particles were well distributed and dispersed in the matrix, although some small clusters 100–300 nm remain in the microstructure. It is believed that strong mechanical bonding made between Al and  $\text{Al}_2\text{O}_3$  particles by using ball mill and press, helps to disperse them more uniformly in the liquid. The  $\text{Al}_2\text{O}_3$  agglomerates reveal that the mentioned bonding between some particles was weakened during the process.

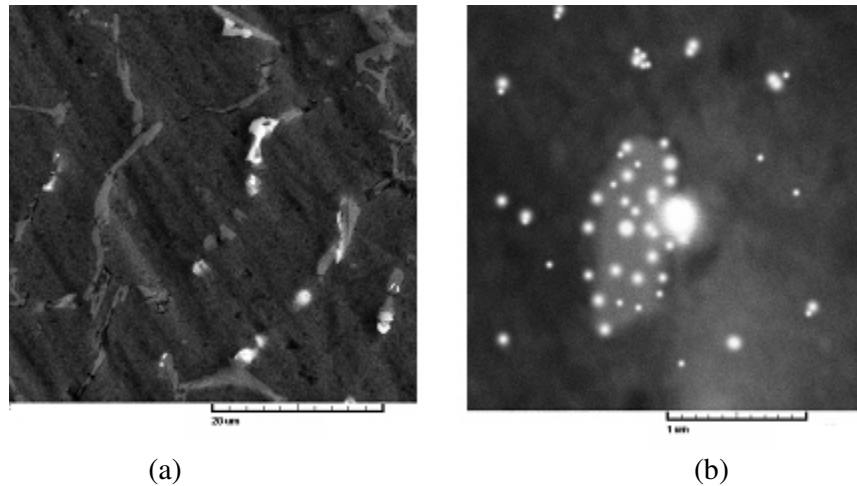


Figure 1: Typical SEM image of nano-composites: (a)  $\text{Al}_2\text{O}_3$  agglomerates, (b) nano-particles dispersion.

In order to verify and determine the composition of the nano-composite, energy dispersion spectrum (EDS analysis) was used. The typical result which is taken from Figure 1(b) is shown in Figure 2. Because the detection zone of EDS beam is bigger than the average size of  $\text{Al}_2\text{O}_3$  particles, the EDS peaks for  $\text{Al}_2\text{O}_3$  nanoparticles will inevitably include compositional information of Al matrix near particles. However, according to the compositional information of matrix, it is evident that Al and O peaks correspond only to composition of nanoparticles.

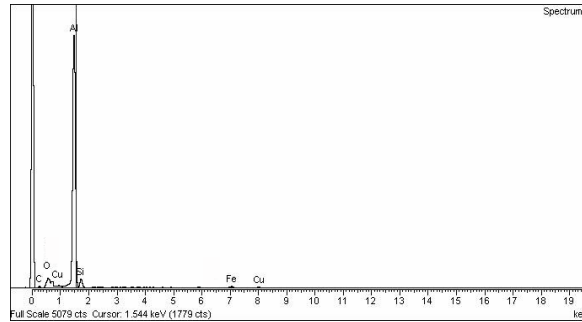


Figure 2: Typical EDS of nano-composites.

The variation in hardness with volume fraction for Al/nanoAl<sub>2</sub>O<sub>3</sub> composites are summarized in Figure 3. Hardness tests were performed on a Brinell hardness machine. For composite materials containing a soft matrix and a hard reinforcing phase, as in the case of particle reinforced composites, the selection of the region in the sample for evaluating the hardness data is very crucial. In order to obtain the average values of hardness, areas predominant in the soft matrix or the hard reinforcing phase should be avoided so that the average values of hardness are attained from these measurements.

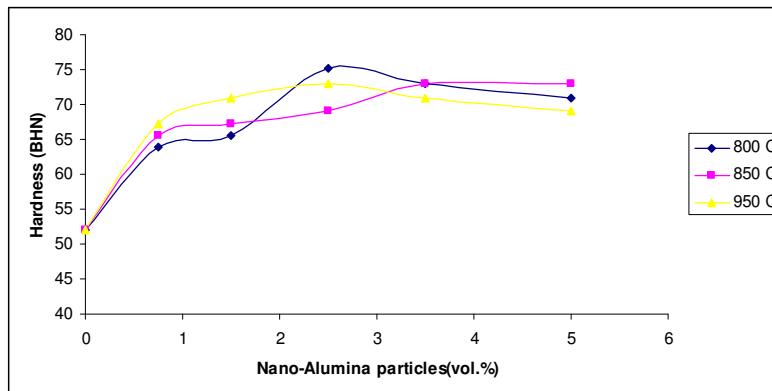


Figure 3: Variation of hardness as a function of vol. % Al<sub>2</sub>O<sub>3</sub> particulates and casting temperature.

It is clear from the graph that the hardness of the composites is higher than that of the non-reinforced alloy. The hardness of the MMCs increases with the volume fraction of particulates in the alloy matrix due to the increasing ceramic phase of the matrix alloy and also increases with decreasing particle size. A significant improvement in both strength and hardness of squeeze cast Al–Si alloy reinforced with alumina and Al alloy reinforced with continuous boron fibres has been reported. The introducing alumina into the Al matrix resulted in increase in mechanical properties [21,22]. The higher hardness of the composites could be attributed to the fact that Al<sub>2</sub>O<sub>3</sub> particles act as obstacles to the motion of dislocation. The hardness increment can also be attributed to reduced grain size. As shown, hardness increases with the amount of Al<sub>2</sub>O<sub>3</sub> present particles.

The dispersion of  $\text{Al}_2\text{O}_3$  particles enhances the hardness, as particles are harder than Al alloy, the material render their inherent property of hardness to the soft matrix [23].

The variation of tensile strength as a function of vol. %  $\text{Al}_2\text{O}_3$  particulates and casting temperature are plotted in figure 4. Assuming perfect bonding and uniform distribution of the particles, and no interaction effect between the deformation of the reinforcing phase and the matrix, the simplest approach to predict the deformation behaviour of composite is through the classical rule of mixtures. But in most of the cases, the strength or ductility obtained from the experimental measurements is noted to be considerably lower than that of the value obtained from the rule of mixture. This is primarily attributed to the existence of thermal mismatch stress generated due to difference in the thermal expansion coefficients between the matrix alloy and the reinforcing phase [24, 25], ineffective load transfer between the phase constituents due to the presence of reaction product, relatively weak bonding, the presence of defects in the reinforcements and the clustering of the particles, etc. [26-29].

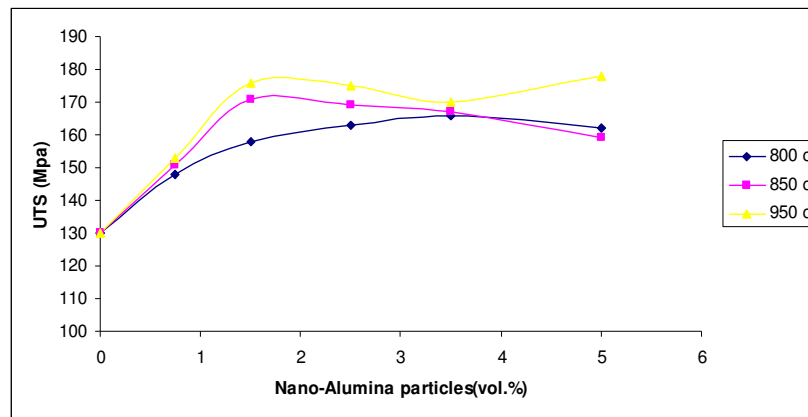


Figure 4: Variation of tensile strength as a function of vol. %  $\text{Al}_2\text{O}_3$  particulates and casting temperature.

It is expected that due to the thermal mismatch stress, there is a possibility of increased dislocation density within the matrix which might lead to making local stress and also increase in strength of the matrix, and thus to the composite. This stress also depends on the temperature from which the composite is cooled. Thus, in the case of casting, the magnitude of thermal mismatch stress is expected to be considerably higher as in this case composite is cooled from its liquid stage. In case of composites, the plastic flow of matrix is constrained due to the presence of these rigid and very strong  $\text{Al}_2\text{O}_3$  particles. The matrix could flow only with the movement of  $\text{Al}_2\text{O}_3$  particle or over the particles during plastic deformation. While  $\text{Al}_2\text{O}_3$  content is significantly higher, the matrix gets constrained considerably to the plastic deformation because of smaller inter-particle distance and thus results in higher degree of improvement in flow stress. It has been understood that the plastic flow of the composite is due to the plastic flow of the matrix. The strain-hardening of the composite is primarily due to hardening of the matrix during its plastic flow. The strain-hardening of matrix is expected to be influenced by the dislocation density and dislocation-to-dislocation interaction and also constraint of plastic flow due to resistance offered by  $\text{Al}_2\text{O}_3$  particles. The dislocation density in the

matrix of the composite might be increasing with increase in  $\text{Al}_2\text{O}_3$ . Similar fact is also true for plastic constraint to the matrix due to particle addition. This is the reason of increase in UTS with adding  $\text{Al}_2\text{O}_3$  content. It may also be noted that a significant amount of dislocation, generated due to the thermal mismatch stress or due to the plastic incompatibility, gets neutralized due to the presence of incoherent weak interface between the particle and the matrix, and micro-porosities in the matrix. The amount of interface area increases with increase in  $\text{Al}_2\text{O}_3$  content and the micro-porosities also increase with increase in  $\text{Al}_2\text{O}_3$  content which might lead to lower flow stress in composite. These factors neutralize their effect towards flow stress and thus composite containing 5 vol. %  $\text{Al}_2\text{O}_3$  exhibits almost the same UTS as that of the 2.5vol%.

Significant combination of increment in UTS and ductility of monolithic aluminum due to presence of nano- $\text{Al}_2\text{O}_3$  as reinforcement (table 1) can primarily be attributed to coupled effect of increase in grain boundary area due to grain refinement, the strong multidirectional thermal stress at the Al/ $\text{Al}_2\text{O}_3$  interface induced by the large difference of coefficient of thermal expansion between matrix and reinforcement, and the effective transfer of applied tensile load to the uniformly distributed enormous number of well bonded strong nano- $\text{Al}_2\text{O}_3$  particulates [30,31].

Table 1. Typical results of mechanical properties and grain morphology.

Materials	Casting at	UTS, MPa	Ductility, %	Grain size, $\mu\text{m}$
Al/1.5Al <sub>2</sub> O <sub>3</sub> without using Al particles	850 °C	126 ±4	1.3	45
Al/1.5Al <sub>2</sub> O <sub>3</sub> using Al particles	850 °C	173±2	2.2	12
Al/2.5Al <sub>2</sub> O <sub>3</sub> using Al particles	850 °C	171±2	2	15
Al/5Al <sub>2</sub> O <sub>3</sub> using Al particles	850 °C	160±3	1.7	15

## 6. CONCLUSIONS

1- Nano-sized  $\text{Al}_2\text{O}_3$  particles reinforced aluminum composites were fabricated by stir casting with the help of micro-Al particles mixing. Grain refinement, reasonably uniform distribution of reinforcement particulates, and the presence of minimal porosity in the composite microstructure indicate suitability of processing used in the present study. It is suggested from the study of microstructural characterization that, nanoparticles are almost uniformly distributed in the matrix, although some small clusters still exist in matrix.

2- EDS analysis indicates that the Al and O elements exist at nanoparticles places.

3- The hardness, UTS and ductility of nano- $\text{Al}_2\text{O}_3$  reinforced aluminium composites improved with the increase in volume fraction of nanoparticles. The maximum hardness was observed in composite including 2.5 vol. %  $\text{Al}_2\text{O}_3$  and cast at 800°C.

## REFERENCES

- [1] G.S. Hanumanth and G.A. Irons, *J. Mater. Sci.*, **28** (1993), pp. 2459–2465.
- [2] Y. Sahin and S. Murphy, *J. Mater. Sci.*, **34** (1996), pp. 5399–5407.
- [3] B. Venkataraman and G. Sundararajan, *Wear*, **245** (2000), pp. 1-2.
- [4] Y. Iwai, T. Honda, T. Miyajima, Y. Iwasaki, M.K. Surappa and J.F. Xu, *Composites Sci. Technol.*, **60** (2000), pp. 1781–1789.
- [5] M. Vedani, F. D’Errico and E. Garibaldi, *Composites Sci. Technol.*, **66** (2006), pp. 343–349

- [6] R. Couturior, D. ducret, P. Merle, J.P. Disser and P. Joubert, *J. Eur. Ceram. Soc.*, **17** (1997), pp. 1861–1866.
- [7] S.C. Lim, M. Gupta, L. Ren and J.K.M. Kwok, *J. Mater. Process. Technol.*, **89–90** (1999), pp. 591–596
- [8] D.P. Mondal, S. Das and R.N. Rao, *Mater. Sci. Eng. A*, **402** (2006), pp. 307–319.
- [9] M. Gui and S.B. Kang, *Mater. Lett.*, **46** (2000), pp. 296–302.
- [10] B.G. Kim, S.L. Dong and Su.D. Park, *Mater. Chem. Phys.*, **72** (2001), pp. 42–47.
- [11] D.P. Mondal and S. Das, *Tribol. Int.*, **39** (2006), pp. 470–478.
- [12] P. Yu, Z. Mai and S.C. Tjong, *Mater. Chem. Phys.*, **93** (2005), pp. 109–116.
- [13] I.G. Watson, M.F. Forster, P.D. Lee, R.J. Daswood, R.W. Hamilton and A. Chirazi, *Composites A*, **36** (2005), pp. 1177–1187.
- [14] T.S. Srivatsan and J. Mattingly, *J. Mater. Sci.*, **28** (1998), pp. 611–620.
- [15] T.S. Srivatsan and T.A. Place, *J. Mater. Sci.*, **14** (1989), pp. 1543–1551
- [16] K. Akio, O. Atsushi, K. Toshiro and T. Hiroyuki. *J. Jpn. Inst. Light Met.*, **49** (1999), pp. 149–154.
- [17] K.M. Mussert, W.P. Vellinga, A. Bakker and S. Van Der Zwaag. *J. Mater. Sci.*, **37** (2002), pp. 789–794
- [18] D.M. Lee, B.K. Suh, B.G. Kim, J.S. Lee and C.H. Lee, *Mater. Sci. Technol.*, **13** (1997), p. 590.
- [19] V. Laurent, P. Jarry, G. Regazzoni and D. Apelian, *J. Mater. Sci.*, **27** (1992), p. 447.
- [20] R.A. Saravanan and M.K. Surappa, *Mater. Sci. Eng.*, **A276** (2000), p. 108.
- [21] P.S. Cooke and P.S. Werner, *Mater. Sci. Eng.*, **A144** (1991), pp. 189–193.
- [22] M. Kok, Ph.D. Thesis, The Institute of Science and Technology of Elazig University, Turkey, 1999
- [23] A.K. Banerjee, P.K. Rohatgy, W. Reif, 1985, Strausbourg, France, November 1985.
- [24] M.C. Watson and T.W. Cline, *Acta Metall. Mater.*, **40** (1992), pp. 135–140.
- [25] J. Llorca, *Comprehensive*, p. 91.
- [26] J. Llorca, A. Martin, J. Ruiz and Mliices, *Metall. Trans. A.*, **24A** (1993), pp. 1575–1588.
- [27] T.J. Dwnes and J.E. King, *Metal Matrix Composites: processing, microstructure and properties*, Riso National Laboratory, Roskilde, Denmark (1991) pp. 305–310.
- [28] J. Llorca and P. Poza, *Mater. Sci. Eng. A*, **A185** (1994), pp. 25–37.
- [29] P.M. Mummery, P. Anderson, G.R. Davis, B. Derby and J.C. Elliott, *Scr. Metall. Mater.*, **29** (1993), pp. 1457–1462.
- [30] R. E. REED-HILL, 2nd edn, 192-194, 267 and 753; 1964, new york, D. Van nostrand.
- [31] A. L. GEIGER and J. A. WALKER; *J. Met.*, 1991, 43, 8-15.